INFLUENCE OF OPENING OF ELECTRONIC EXPANSION VALVE ON HEATING PERFORMANCE OF VEHICLE HEAT PUMP SYSTEM WITH ECONOMIZER

by

Haijun LI*, Gang CHEN, Zhiyong SU, Yibo ZHANG, Jiayang GAO, Ruikai NIU, Long CHENG, and Shuguang YIN

School of Smart Energy and Environment, Zhong yuan University of Technology, Zhengzhou, China

Original scientific paper
https://doi.org/10.2298/TSCI2602993L

The objective of this study was to investigate the impact of the electronic expansion valve opening in an automotive heat pump system with an economizer on the system winter heating performance and frost-related characteristics. The experiments were conducted at a temperature of –10 °C during the winter months. The adjustment of the opening degrees of the main and complementary electronic expansion valve was implemented to facilitate an analysis of the heating performance parameters and the alterations in frost formation and melting. The findings demonstrated that a diminution in the main circuit electronic expansion valve opening from 40% to 24% resulted in an augmentation of the exhaust gas temperature by 12.24 °C, accompanied by a maximum heat production of 2.837 kW and a COP of 1.99. In the low pressure makeup mode, an increase in the makeup electronic valve opening from 8% to 15% resulted in a 7.27 °C decrease in the exhaust gas temperature. Concurrently, the maximum heat production and the COP reached 2.851 kW and 2, respectively. In the medium pressure makeup mode, an increase in the makeup electronic valve opening from 8% to 20% resulted in a 9.4 °C reduction in the exhaust temperature. This adjustment resulted in a maximum heat production of 3.235 kW and a COP of 1.96. In consideration of the subject of frost-related phenomena, the following observations were made: the duration required to execute frosting in the no-makeup gas, low pressure makeup gas, and medium pressure makeup gas modes was 82 minutes, 90 minutes, and 95 minutes, respectively. The duration required for frost melting was determined to be 5 minutes and 20 seconds, 4 minutes and 30 seconds, and 3 minutes, and 56 seconds, respectively. These findings offer significant insights into the optimization of automotive heat pump systems during winter operations.

Keywords: *heat pump, electronic expansion valve, heating production, frost formation and melting*

Introduction

In recent years, the development of pure electric vehicles has gained significant momentum due to their distinct environmental advantages, which are in full compliance with global sustainable development strategies [1, 2]. The Kigali Amendment to the Montreal Protocol has imposed a substantial restriction on the use of refrigerants with a high global warm-

* Corresponding author, e-mail: haijun_li007@126.com

ing potential (GWP > 150) [3]. Consequently, the novel R1234yf refrigerant, characterized by its low GWP of merely 4 and its physical resemblance to the extensively utilized R134a refrigerant [4], has materialized as a compelling substitute within the domain of automotive air conditioning.

Nonetheless, the heat pump air-conditioning system in pure electric vehicles is a significant energy-consuming component, second only to the drive system [5]. The high energy consumption of electric vehicles poses a significant challenge to their widespread adoption, as it severely limits their driving range [6]. The electronic expansion valve (EEV) [7], characterized by its rapid response, precise control, and wide adjustment range, plays a crucial role in regulating the refrigerant flow within the heat pump system. Nonetheless, during periods of winter low temperatures, inadequate EEV opening settings may result in a series of complications, including a reduction in heating performance and an escalation in energy consumption. Consequently, the enhancement of the system heating performance while optimizing electric vehicle operation has emerged as a primary research focus [8].

A substantial corpus of research has been amassed through previous studies, which have made important contributions to the understanding of the heat pump system. Xu *et al.* [9] investigated the heat pump air-conditioning system and determined that the make-up gas technology exhibited superior cooling performance in comparison to conventional heat pump systems. Beghi and Cecchinato [10] experimentally determined the knowledge base and control rules for superheat control in heat pump systems by adjusting the EEV. Zhang *et al.* [11] proposed a staged control strategy for the EEV based on the minimum stable superheat curve to effectively improve the system energy efficiency ratio. Wang's *et al.* [12] investigation focused on the performance of a CO_2 heat pump air conditioning system, emphasizing the necessity for the EEV opening to take into account critical factors such as exhaust gas temperature and suction superheat. Zou *et al.* [13] discovered that altering the EEV opening could cause subsequent changes in key parameters of the heat pump system, such as superheat, COP, and condensing temperature.

Furthermore, a considerable number of researchers have devoted their efforts to the study of frost-related issues in heat pump systems. A multitude of scholars have undertaken exhaustive research endeavors to address the challenges posed by frost delay and efficient defrosting. These studies have delved into the intricacies of frost growth mechanisms and the characteristics associated with defrosting processes [14, 15]. For instance, a hierarchical modeling approach of droplet growth during the initial stage of frosting has demonstrated a close relationship between the growth rate and substrate temperature as well as air humidity, with the growth rate increasing in proportion to decreases in substrate temperature and increases in air humidity [16]. In the context of heat pump air conditioning systems, the accumulation of frost on the evaporator component at low operational temperatures has been observed to result in a substantial diminution of heat transfer efficiency, with the magnitude of this reduction reported to range from 50% to 75% [17]. A number of studies have been conducted on the subject of EEV control schemes. For instance, as reported in [18], the efficacy of defrosting processes can be augmented by regulating the opening of the EEV. Study by Liu *et al.* [19] examined the frost formation characteristics in a quasi-secondary compression system with make-up gas enthalpy increase under various working conditions. The study found a relatively small error between the actual defrosting amount and the *theoretical optimal defrosting amount* calculated by the semi-empirical formula.

Despite the valuable research efforts in this area, the majority of extant literature focuses on improving heating performance through system control strategies, often overlooking

the combined effects of frosting and defrosting on the overall system performance. Furthermore, there is a paucity of in-depth research on determining the optimal EEV opening under –10 °C conditions and its impact on heating performance, as well as on the frost and defrost characteristics.

The present study established an experimental set-up for an automotive heat pump air conditioning system with an economizer. This system is based on the principle of a quasi-secondary compression cycle and utilizes the R1234yf refrigerant. The reverse cycle defrosting method was utilized in this process. The primary objectives of this study were twofold: first, to conduct a comprehensive analysis of the influence of the opening degrees of the main circuit and make-up EEV on parameters such as exhaust temperature, compressor power, heat production, and COP. Second, to explore the impact of the optimal EEV opening on frosting and defrosting processes in different make-up gas modes. The objective of this research is to facilitate a more comprehensive understanding of the system's behavior under low temperature conditions. Additionally, it aims to offer practical guidance for optimizing the operation of automotive heat pump systems during winter.

Experimental set-up

As illustrated in fig. 1, the system circulation principle is comprised of both main and supplementary circuits, which collectively define its heating cycle. The main circuit functions are: First, the compressor transforms high temperature and high pressure gaseous refrigerants into four-way valves. These valves direct the refrigerants through the condenser and one-way valve. The refrigerants then pass through liquid storage and a filter drier before reaching the economizer, where they release part of the heat. Subsequently, the main circuit EEV throttles. The low temperature and low pressure gas-liquid two-phase refrigerants in the condenser absorb the heat and return to the compressor. The makeup circuit is defined as the sequence of events that occurs subsequent to the economizer, wherein the flow progresses through the throttling pressure reduction of the complementary EEV. In the second instance,

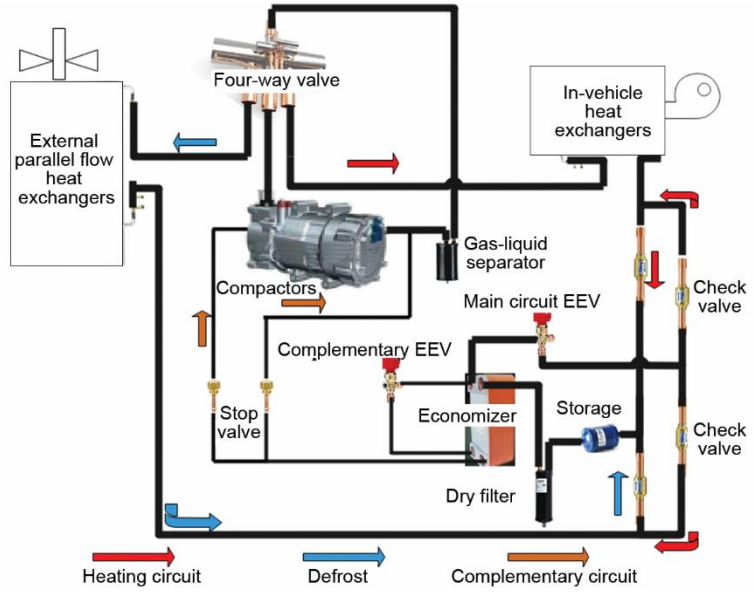

Figure 1. System circulation principle

the economizer absorbs the heat from the condenser refrigerant. The refrigerant that has been made up for the heat exchange then flows back to the compressor after mixing with the refrigerant of the main circuit. This increases the mass-flow rate of the refrigerant entering the next cycle. In the context of low pressure make-up gas, the make-up refrigerant is introduced in proximity to the compressor suction port, where it undergoes a mixture with the refrigerant emanating from the evaporator. This mixture subsequently enters the compressor. In medium pressure make-up gas mode, the make-up refrigerant is located in the compressor first compression chamber, situated at the rear of the movable vortex disc and the fixed vortex disc sealing at the movable vortex disc. This configuration facilitates the mixing of the refrigerant with the main road during the make-up process, thereby ensuring adequate compression. The operation of the cut-off valve is governed by the opening and closing control of low pressure and medium pressure make-up gas modes.

Experimental equipment

The experimental bench is constructed in accordance with the structural characteristics of the heat pump air conditioning for pure electric vehicles and the principle of quasi-stage compressor with economizer. The refrigerant utilized in the experimental bench is R1234yf, which is divided into three sections: the heat exchanger outside the vehicle, the experimental equipment, and the heat exchanger inside the vehicle, as illustrated in fig. 2(a). The primary parameters of the experimental prototype and the test instrument are enumerated in tab. 1. The experiment utilized the main circuit EEV and the complementary circuit EEV for CAREL E2V-24 and E2V-14, as illustrated in physical fig. 2(b). The equipment parameters are outlined in tab. 2. The opening and closing of the charge port of a make-up type compressor is controlled by a shut-off valve, see fig. 2(c).

Table 1. Main parameters of the experimental prototype and test instruments

Equipment name	Specifications
Compressor	HIGHLY variable frequency vortex EVS36. Refrigerant: R134yf. Operating range: 1500~6000 rpm. Displacement: 36 (cc/rev). Rated voltage: DC350~750V. Cooling capacity: 6.5 kW. Refrigerating oil: HAF68. Applicable environment: –40~80 °C
External parallel flow heat exchanger	Zheng Zhou Kelin. Size: 900 × 415 × 25.9 mm. Number of flow: 2. Number of flat tube rows: 44. Heat exchange area: 2.07 m^2
Parallel flow heat exchanger in car	Zheng Zhou Kelin. Size: 585 × 285 × 25.9 mm. Number of flow: 1. Number of flat tube rows: 24. Heat exchange area: 1.40 m^2
Outside fan	Shanghai Dedong FAD60-4 axial fan. Rated power: 60 W. Impeller speed 1400 rpm. Rated air volume: 8700 m^3/h. A (machine)
Interior fan	Variable frequency centrifugal fan from Ebm-K3G097. Rated air volume: 1200 m^3/h. Voltage DC: 26V. A (machine)
Intermediate heat exchanger	Weal Yield (Jiangsu) plate heat exchanger model B3-014-20D-3.0. Design capacity: 6.06 kW. Design pressure: 3.0 MPa. Design temperature: –160~200 °C
Four-way valve	Dunan DSF-20. Applicable capacity: 7.1~25 kW

Table 2. The EEV parameters

Name	Model number	Rated cooling capacity [kW]	Adjustment range
Main circuit EEV	CAREL E^2V-24	16.3	10~100%
Complementary EEV	CAREL E^2V-14	5.7	0~100%

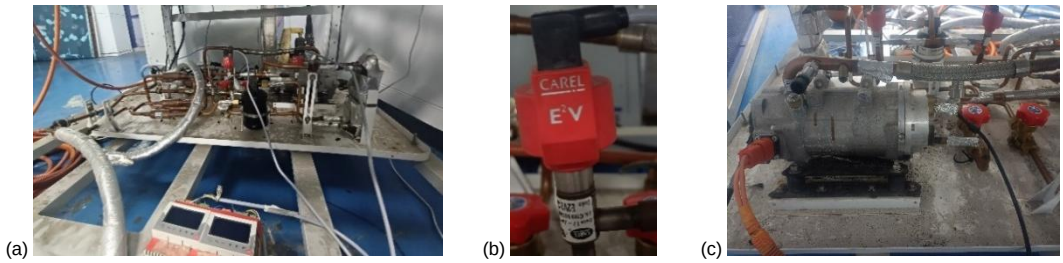

Figure 2. Experimental set-up object; (a) system lab bench, (b) EEV, and (c) electric scroll compressors

Test condition

Experiments were conducted in a standard enthalpy difference laboratory, where the ambient temperature outside the vehicle was set at –10 °C and the ambient temperature inside the vehicle was set at 20 °C. The air enthalpy difference was utilized to assess the performance parameters of the automotive heat pump system. The charge of R1234yf refrigerant was 1.632 kg, and the compressor speed was set at 3600 rpm. In both the heating and frost conditions, the air volume inside the vehicle is 1200 m³/h, while the air volume outside the vehicle is 7830 m³/h. The defrosting process was executed through the utilization of the reverse cycle method, employing an airflow of 540 m³/h within the vehicle and 7830 m³/h in the external environment. The temperature of the heat exchanger, both during evaporation and condensation, was documented by means of an infrared thermographic camera. The specific experimental test conditions are delineated in tab. 3.

Table 3. Experimental test conditions

Working condition	Main circuit EEV opening [%]	Complementary EEV opening [%]	Make-up gas modes	Running time [minutes]
Heating condition	24, 29.5, 34.5, 40	–	No make-up gas	–
	34.5	8, 10, 12, 15	Low pressure make-up gas	
	34.5	8, 10, 12, 15, 20	Middle-pressure make-up gas	
Frost condition	34.5	–	No make-up gas	5, 15, 30, 60, 90, 120, 150
	34.5	10	Low pressure make-up gas	
	34.5	10	Middle-pressure make-up gas	
Frost melting condition	34.5	–	No make-up gas	–
	34.5	10	Low pressure make-up gas	
	34.5	10	Middle-pressure make-up gas	

Experimental analysis

As illustrated in fig. 3, the augmentation in the EEV opening exhibits a downward trend in exhaust temperature and an upward trend in compressor power. An experiment was conducted to investigate the effects of increasing the main circuit EEV opening from 24% to 40% in the no make-up gas mode on the compressor discharge temperature. The results showed a significant reduction in the discharge temperature from 90.79-78.55 °C, indicating a substantial decrease of 12.24 °C. The augmentation in compressor power from 1.364-1.364 kW yielded a diminution of 76 W, which exerted a negligible influence on compressor power. In the absence of makeup gas, the augmentation of the primary circuit EEV opening and the diminution of the exhaust temperature are predominantly attributable to the escalation of the mass-flow rate of the refrigerant on the low pressure side and the augmentation of the mass-flow rate of the refrigerant entering the evaporator. This enhances the effective heat exchange area of the evaporator, consequently reducing the evaporation temperature. Concurrently, the temperature of the refrigerant entering the suction port of the compressor declines, resulting in the reduction of the exhaust temperature. The observed rise in compressor power is attributable to the augmented refrigerant flow into the compressor suction port. The primary circuit EEV opening was set at 34.5%, and the complementary EEV opening was increased from 8% to 15% in the low pressure make-up gas mode. Consequently, the compressor discharge temperature was reduced from 71.23-63.96 °C, resulting in a 7.27 °C reduction in the discharge temperature. Concurrently, the compressor power increased from 1.423-.429 kW, giving it a 6 W increase. The augmentation in the opening of the complementary EEV in the low pressure mode has been demonstrated to engender an increase in the heat exchange between the make-up refrigerant and the main refrigerant entering the economizer. This, in turn, has been shown to result in a reduction in the main refrigerant superheat and the compressor discharge temperature. The total refrigerant mass-flow rate on the low pressure side remains constant, and the compressor power undergoes minimal change. When the main circuit EEV opening was set at 34.5% and the complementary EEV opening was increased from 8% to 20% in the medium pressure make-up gas mode, the compressor discharge temperature was reduced from 75.15-65.75 °C, resulting in a 9.4 °C reduction in the discharge temperature. The compressor power has been augmented from 1.635-1.681 kW, marking an increase of 46 W in compressor power. In the medium pressure make-up gas mode, the complementary EEV opening has been observed to increase, concurrently with a decrease in the discharge temperature. The make-up

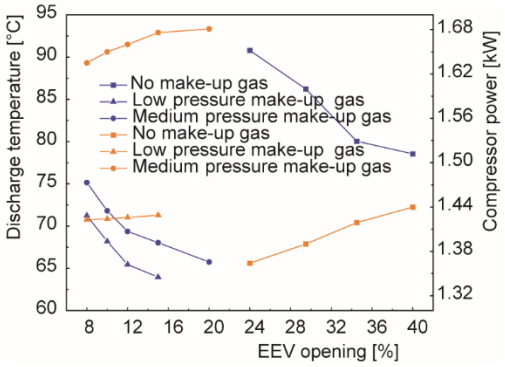

Figure 3. The effect of EEV opening on discharge temperature and compressor power

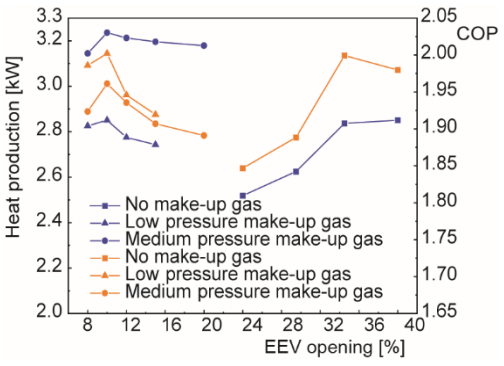

Figure 4. The effect of EEV opening on heat production and COP

circuit refrigerant has been found to absorb more heat from the main circuit refrigerant, thereby reducing the compressor discharge temperature.

As illustrated in fig. 4, increasing the EEV opening results in an initial increase in the COP, followed by a subsequent decrease. Additionally, the heat production in the three modes exhibits distinct trends. In the absence of makeup gas mode, an augmentation in the main circuit EEV opening from 24% to 40% results in an escalation in heat production from 2.519-2.851 kW, thereby inducing an increase of 332 W. Concurrently, the COP undergoes an enhancement from 1.85-1.98. The maximum values of COP and heat production appear to be 1.99-2.837 kW at 34.5% main circuit EEV opening. In the absence of makeup gas mode, the augmentation of the primary circuit EEV opening results in an escalation of the mass-flow of refrigerant on the low pressure side and an increase in the mass-flow of refrigerant into the evaporator. This enhancement in refrigerant flow leads to an improvement in heating capacity and an increase in the COP. Subsequent to the primary circuit's opening at 34.5%, the effective heat transfer area of the evaporator approaches saturation. Concurrently, the heat production undergoes a gradual increase, with the rise in compressor power assuming a predominant role. This phenomenon results in a decline in the COP. In the low pressure make-up gas mode, the heat production decreased from 2.826-2.743 kW and the COP decreased from 1.98 to 1.92 when the main circuit EEV opening was set at 34.5% and the complementary EEV opening was increased from 8% to 15%.

When the complementary EEV opening is set at 10%, the maximum values of the heat production and COP appear to be 2.851 kW and 2, respectively. The primary refrigerant in the economizer is absorbed by the make-up refrigerant, leading to a reduction in evaporator inlet temperature and an enhancement in heat production. Consequently, the COP increases. The complementary EEV opening persists in opening up, the compressor power assumes a dominant role, and the COP declines. The primary circuit EEV opening is set at 34.5%, and when the complementary EEV opening is elevated from 8% to 20% in the medium pressure make-up gas mode, the heat production increases from 3.145-3.179 kW, and the COP decreases from 1.93 to 1.89. When the complementary EEV opening is at 10%, the maximum values of heat production and COP appear to be 3.236 kW and 1.96, respectively. The EEV opening is increased from 8% to 10%, which is indicative of an upward trend in heat production. Consequently, the COP is increased. The complementary EEV opening persists, with the compressor power assuming a predominant role, resulting in a decline in the COP. The heating capacity in medium pressure make-up gas mode is larger than that in the other two modes, which effectively solves the situation of insufficient heating capacity under low temperature working conditions.

As illustrated in fig. 5, the evaporation temperature demonstrates a gradual decrease in accordance with an increase in the duration of operation across the three distinct modes. Following a 90 minute operation period, the evaporation temperature typically attains stability. The evaporation temperature was recorded from five minutes after switching on, and the results demonstrated a decrease from –13.25–-29.1 °C in no make-up gas mode, from –12.79-28.19 °C in low pressure make-up gas mode, and from –12.05–-27.51 °C in medium pressure make-up gas mode. The lowest evaporation temperature is observed when the frost is stabilized in the no make-up gas mode. Conversely, the evaporation temperature in the low pressure make-up gas mode is higher than that in the no make-up gas mode, and the evaporation temperature in the medium pressure make-up gas mode is the highest. In conditions characterized by low temperatures, the evaporation temperature of the evaporator can be effectively increased through the implementation of gas replenishment. The medium pressure make-up

gas mode has been found to exhibit the smallest rate of evaporative temperature reduction. The most rapid decline in evaporative temperature is observed in the no make-up gas mode, which prolongs the evaporator frost cycle.

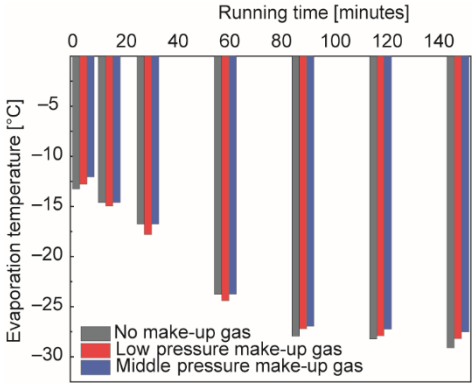

Figure 5. The effect of running time on evaporation temperature

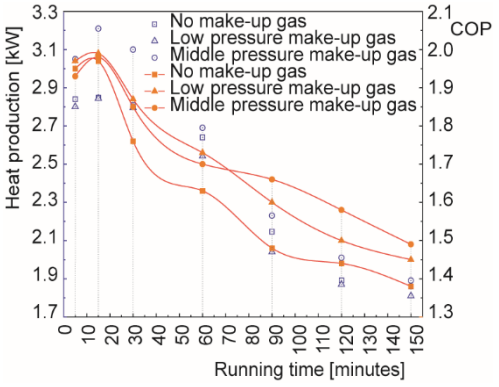

Figure 6. The effect of running time on heat production and COP

As the duration of operation increases, the heat production in the three operating modes gradually decreases, while the COP first increases and then decreases, see fig. 6. In the initial phase of frost, the COP is approximately equal, and the heat production is maximum in the medium pressure make-up gas mode. This is superior to the other two modes, and the effective make-up gas mode reduces the exhaust temperature of the system and improves its performance. The heat production decreased from a maximum of 2.848-1.859 kW, representing a 52.77% decrease, and the COP decreased from a maximum of 1.97 to 1.38, indicating a 42.75% decrease, as the operating time was extended in the no make-up gas mode. In the low pressure make-up gas mode, the heat production decreased from a maximum of 2.844-1.81 kW, representing a 57.13% decrease, and the COP decreased from a maximum of 1.99 to 1.45, indicating a 37.24% decrease, as the operating time was prolonged. In the medium pressure make-up gas mode, an extension of the running time resulted in a decrease in heat production from a maximum of 3.21-1.89 kW, representing a reduction of 61.38%. Concurrently, the COP decreased from a maximum of 1.98 to 1.49, indicative of a reduction of 32.89%. Once the system has been stabilized, the medium pressure make-up gas mode demonstrates the highest levels of heat production and COP. This configuration is optimal for meeting the demand for winter heating, thereby effectively prolonging the system's frost time.

As illustrated in fig. 7, the system is initiated at the end of the frost formation process in all three modes. The fastest completion time is observed in the low pressure make-up gas mode, with an average of 82 minutes. The medium pressure make-up gas and high pressure make-up gas modes demonstrate an extended completion time, with the medium pressure make-up gas mode exhibiting the slowest time of 95 minutes under low temperature conditions. This is primarily attributable to the low temperature heat pump air-conditioning system with economizer, which effectively raises the evaporation temperature and prolongs the frost cycle by means of the effective make-up gas mode.

As illustrated in fig. 8, the average condensing temperature and frost melting time during the frost melting process exhibit variability for various make-up gas modes. The average condensing temperature of the system can be increased and the defrosting time can be re-

duced by using the two make-up gas modes. The medium pressure make-up gas mode has been shown to have the highest average condensing temperature and the shortest frost melt time. The medium pressure make-up gas mode exhibits a high make-up circuit refrigerant flow rate and a high heat exchange with the main circuit refrigerant in the economizer. The subcooling degree in front of the main circuit EEV is increased, the liquid refrigerant flowing into the evaporator is augmented, the heat exchange of the evaporator is intensified, and subsequently, the heat exchange of the condenser is reinforced. This results in an elevated condensing temperature and a reduced frost melting time.

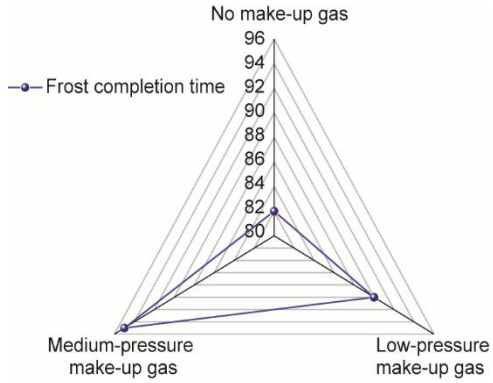

Figure 7. The effect of make-up gas modes on frosting

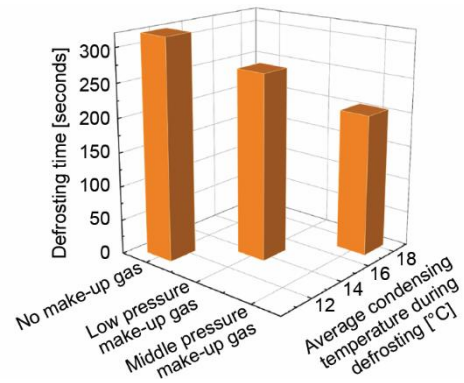

Figure 8. The effect of make-up gas modes on frost melting

Conclusions

In the context of an automotive heat pump system equipped with an economizer that has undergone testing at a temperature of –10 °C, it has been observed that varying adjustments to the EEV opening result in a spectrum of heating performance outcomes. A reduction in the main circuit EEV opening from 40% to 24% results in an increase of 12.24 °C in exhaust gas temperature, and the maximum heat production and COP reach 2.837 kW and 1.99, respectively. In the low pressure make-up gas mode, an increase in the complementary EEV opening from 8% to 15% results in a 7.27 °C decrease in exhaust gas temperature, with maximum heat production and a COP of 2.851 kW. In the medium pressure make-up gas mode, an increase in the complementary EEV opening from 8% to 20% results in a 9.4 °C decrease in exhaust temperature. Concurrently, the maximum heat production and COP reach 3.235 kW and 1.96, respectively. Specifically, in the no make-up gas mode, the optimal main circuit EEV opening is 34.5%. In both the low pressure and medium pressure make-up gas modes, the optimal main circuit EEV opening is 34.5%, and the optimal complementary EEV opening is 10%.

As the operation time extends in the three different modes, the make-up gas modes, especially the medium pressure make-up gas mode, exhibit significant advantages. These advantages are a result of the optimal EEV openings (34.5% for the main circuit and 10% for the complementary circuit). These modes have been shown to effectively increase the evaporating temperature and heat production, and prolong the evaporator frost cycle. The medium pressure make-up gas mode exhibits the highest evaporating temperature, the greatest heat production, and the longest duration (95 minutes) required to complete frosting. This is ad-

vantageous for sustaining the system's efficacy during the heating process and postponing the onset of frosting.

At a temperature of –10 °C, the reverse cycle defrosting method, operating in three distinct modes with optimal EEV openings, was found to yield the highest average condensing temperature and the shortest defrosting time (3 minutes and 56 seconds) when employing the medium pressure make-up gas mode. This finding suggests that the implementation of effective makeup gas modes can enhance the defrosting efficiency, thereby ensuring the rapid and efficient defrosting of the system. Consequently, this enhances the overall heating performance and reliability of the automotive heat pump system during winter.

Looking ahead, AI-based thermal science [20] will revolutionize heat management *via* deep learning for intelligent systems, optimize heat exchangers through AI-driven design, and advance micro/nanofluids and fractal thermal modeling. Meanwhile, differential equation-driven intelligent control [21] integrates AI, quantum computing, and adaptive strategies, using physics-informed neural networks for PDE solving and quantum-enhanced algorithms for SDE optimization. It aims to create self-evolving industrial systems, such as smart grids and robotic arms, enabling real-time, multi-scale control for Industry 5.0. Both fields drive innovation at the intersection of AI and physical sciences, fostering sustainable and intelligent technological ecosystems.

Reference

[1] Donateo, T., *et al.* A Method to Estimate the Environmental Impact of an Electric City Car during Six Months of Testing in an Italian City, *Journal of Power Sources*, *270* (2014), 1, pp. 487-498
[2] Zhuang, X., Jiang, K., Research on the Development Roadmap of Pure Electric Vehicles in China, *Automotive Engineering*, *34* (2012), 2, pp. 91-97
[3] Liu, B., *et al.* Seasonal Performance Analysis of a Heat Pump with a New R134a Replacement Medium, *Journal of Engineering Thermophysics*, *43* (2022), 12, pp. 3177-3183
[4] Celil, A. M., *et al.*, Performance Evaluation of an Automotive Air Conditioning and Heat Pump System Using R1234yf and R134a, *Science and Technology for the Built Environment*, *27* (2021), 1, pp. 44-60
[5] Kwon, C., *et al.*, Performance Evaluation of a Vapor Injection Heat Pump System for Electric Vehicles, *International Journal of Refrigeration*, *74* (2016), 1, pp. 138-150
[6] Zhang, Z., *et al.*, The Solutions to Electric Vehicle Air Conditioning Systems: A Review, *Renewable and Sustainable Energy Reviews*, *91* (2018), 1, pp. 443-463
[7] Zheng, S., *et al.* Numerical and Experimental Study on Cavitation and Noise Characteristics of Electronic Expansion Valve, *Sci. Rep., 15* (2025), 13499
[8] Abdullah, M., *et al.,* Electric Vehicle Battery Temperature Control Using Fuzzy Logic, *Aut. Control Comp. Sci. 58* (2024), June, pp. 237-251
[9] Xu, X., *et al.*, Refrigerant Injection for Heat Pumping/Air Conditioning Systems: Literature Review and Challenges Discussions, *International Journal of Refrigeration*, *34* (2010), 2, pp. 402-415
[10] Beghi, A., Cecchinato, L., A Simulation Environment for Dry-Expansion Evaporators with Application to the Design of Autotuning Control Algorithms for Electronic Expansion Valves, *International Journal of Refrigeration*, *32* (2009), 7, pp. 1765-1775
[11] Zhang, M., *et al.,* Research on an Adaptive Segmented Electronic Expansion Valve Control Strategy, *Fluid Machinery*, *48* (2020), 6, pp. 14-19
[12] Wang, D. D., *et al.*, Heating Performance Characteristics of CO_2 Heat Pump System for Electrical Vehicle in a Cold Climate, *International Journal of Refrigeration*, *85* (2018), 1, pp. 27-41
[13] Zou, H., *et al.* Experimental Study on Heating Performance of an R1234yf Heat Pump System for Electric Cars, *Energy Procedia*, *142* (2017), 1, pp. 1015-1021
[14] Tian, G., *et al.*, A Review of Condensation Frosting-Mechanisms and Promising Solutions, *Crystals*, *13* (2023), 3, pp. 493-493
[15] Long, Z., *et al.*, Frosting Mechanism and Behaviors on Surfaces with Simple Geometries: A State-of-the-Art Literature Review, *Applied Thermal Engineering*, *215* (2022), 118984

[16] Zhao, W., *et al.,* Laws of Droplet Growth on Superhydrophobic Surfaces at the Early Stage of Frosting, *Journal of Central South University (Natural Science Edition)*, *51* (2020), 1, pp. 231-238
[17] Zhang, L., *et al.,* Simulation Study of Frost Layer Growth at the End of Fins on the Windward Side of a Tube-Fin Heat Exchanger, *Journal of Chemical Engineering*, *74* (2023), S1, pp. 179-182
[18] Qu, M., *et al.,* An Experimental Investigation on Reverse-Cycle Defrosting Performance for an Air Source Heat Pump Using an Electronic Expansion Valve, *Applied Energy*, *97* (2012), Sept., pp. 327-333
[19] Liu, X., *et al.* Study on Theoretical Optimal Defrosting Volume of Quasi-Secondary Compression Air Source Heat Pump with Make-Up Gas and Enthalpy, *Journal of Solar Energy*, *45* (2024), 7, pp. 407-414
[20] Lei, X. H., He, J.-H., Frontiers in Thermal Science Driven by Artificial Intelligence, *Thermal Science*, *29* (2025), 3, Part A, pp. 1671-1677
[21] Cheng, Y., *et al.*, Differential Equation-Driven Intelligent Control: Integrating AI, Quantum Computing, and Adaptive Strategies for Next-Generation Industrial Automation, *Advances in Differential Equations and Control Processes*, *32* (2025), 3096

Paper submitted: October 1, 2024
Paper revised: May 10, 2025
Paper accepted: May 22, 2025
2026 Published by the Vinča Institute of Nuclear Sciences, Belgrade, Serbia.
This is an open access article distributed under the CC BY-NC-ND 4.0 terms and conditions.